TRAP1 regulates the response of colorectal cancer cells to hypoxia and inhibits ribosome biogenesis under conditions of oxygen deprivation

GIUSEPPINA BRUNO[1], VALERIA LI BERGOLIS[1], ANNAMARIA PISCAZZI[1], FABIANA CRISPO[2], VALENTINA CONDELLI[2], PIETRO ZOPPOLI[2], FRANCESCA MADDALENA[2], MICHELE PIETRAFESA[2], GUIDO GIORDANO[1], DANILO SWANN MATASSA[3], FRANCA ESPOSITO[3] and MATTEO LANDRISCINA[1,2]

[1]Medical Oncology Unit, Department of Medical and Surgical Sciences, University of Foggia, I-71122 Foggia; [2]Laboratory of Pre-Clinical and Translational Research, IRCCS, Referral Cancer Center of Basilicata, I-85028 Rionero in Vulture, Potenza; [3]Department of Molecular Medicine and Medical Biotechnology, University of Naples Federico II, I-80131 Naples, Italy

Received February 11, 2022; Accepted April 12, 2022

DOI: 10.3892/ijo.2022.5369

Abstract. Metabolic rewiring fuels rapid cancer cell proliferation by promoting adjustments in energetic resources, and increasing glucose uptake and its conversion into lactate, even in the presence of oxygen. Furthermore, solid tumors often contain hypoxic areas and can rapidly adapt to low oxygen conditions by activating hypoxia inducible factor (HIF)-1α and several downstream pathways, thus sustaining cell survival and metabolic reprogramming. Since TNF receptor-associated protein 1 (TRAP1) is a HSP90 molecular chaperone upregulated in several human malignancies and is involved in cancer cell adaptation to unfavorable environments and metabolic reprogramming, in the present study, its role was investigated in the adaptive response to hypoxia in human colorectal cancer (CRC) cells and organoids. In the present study, glucose uptake, lactate production and the expression of key metabolic genes were evaluated in TRAP1-silenced CRC cell models under conditions of hypoxia/normoxia. Whole genome gene expression profiling was performed in TRAP1-silenced HCT116 cells exposed to hypoxia to establish the role of TRAP1 in adaptive responses to oxygen deprivation. The results revealed that TRAP1 was involved in regulating hypoxia-induced HIF-1α stabilization and glycolytic metabolism and that glucose transporter 1 expression, glucose uptake and lactate production were partially impaired in TRAP1-silenced CRC cells under hypoxic conditions. At the transcriptional level, the gene expression reprogramming of cancer cells driven by HIF-1α was partially inhibited in TRAP1-silenced CRC cells and organoids exposed to hypoxia. Moreover, Gene Set Enrichment Analysis of TRAP1-silenced HCT116 cells exposed to hypoxia demonstrated that TRAP1 was involved in the regulation of ribosome biogenesis and this occurred with the inhibition of the mTOR pathway. Therefore, as demonstrated herein, TRAP1 is a key factor in maintaining HIF-1α-induced genetic/metabolic program under hypoxic conditions and may represent a promising target for novel metabolic therapies.

Correspondence to: Professor Matteo Landriscina, Medical Oncology Unit, Department of Medical and Surgical Sciences, University of Foggia, Viale Pinto 1, I-71122 Foggia, Italy
E-mail: matteo.landriscina@unifg.it

Key words: TNF receptor-associated protein 1, hypoxia, hypoxia inducible factor 1α, glycolysis, ribosome biosynthesis

Introduction

Metabolic rewiring, a cellular mechanism of adaptation to an unfavorable microenvironment, supports the proliferation, survival and long-term maintenance of cancer cells (1). In contrast to non-malignant tissues, tumors are characterized by an increased rate of glycolysis to meet their energy demands even in the presence of oxygen, a phenomenon known as aerobic glycolysis or the Warburg effect (2). Warburg metabolism, consisting of a glucose conversion to lactate even when oxygen is available, has emerged as a hallmark of cancer (3) and metabolic rewiring from glycolysis to oxidative phosphorylation (OXPHOS) and vice versa is responsible for driving cancer progression (4).

Solid tumors often contain a hypoxic area and hypoxia has been shown to lead to a poor prognosis in cancer patients (5), due to its potential to increase malignancy, resistance to treatment and the risk of metastasis (6). The major transcriptional regulator of adaptive responses to hypoxia is the hypoxia inducible factor 1 (HIF-1), a heterodimeric complex composed of HIF-1α and HIF-1β/Aryl hydrocarbon receptor nuclear translocator (7,8). Unlike the β-subunit, which is ubiquitously expressed, the α-subunit is oxygen-sensitive and stabilized under hypoxic conditions. The active form of the HIF-1αβ complex induces the expression of a number of hypoxia-responsive genes by binding to hypoxia response element (HRE) (9), including vascular endothelial growth factor (VEGF) (10)

and several metabolic genes, such as glucose transporter 1 (GLUT1) (11), lactate dehydrogenase A (LDHA) (12,13) and pyruvate dehydrogenase kinase 1 (PDK1) (14,15). This gene expression reprogramming induced by HIF-1α activates angiogenesis and sustains a metabolic rewiring toward Warburg metabolism (10,16). In this complex scenario, a crucial role is played by molecular chaperones in connecting different intracellular pathways (17). TRAP1 is a member of the HSP90 molecular chaperone family, overexpressed in ~60% of human colorectal carcinomas (CRCs), and whose upregulation occurs early in CRC progression; thus, it is hypothesized that it plays a role in the transition from low- to high-grade adenomas (18). TRAP1 can regulate cancer cell adaptation to stress environmental conditions (19-21) and modulate tumor energy metabolism, promoting glycolysis and inhibiting OXPHOS in a context- and tumor-dependent manner (22). In a recent study by the authors, it was reported that TRAP1 favors Warburg metabolism through increased glucose uptake and lactate production and downregulates OXPHOS both in CRC cell lines and CRC patient-derived spheroids (23). Furthermore, TRAP1 binds and inhibits succinate dehydrogenase and cytochrome oxidase (respiratory chain complexes II and IV, respectively) (24,25) with the downregulation of OXPHOS and succinate accumulation. Since succinate stabilizes HIF-1α by blocking prolyl hydrolases and, thus preventing its degradation following ubiquitination, HIF-1α stabilization has been proposed as the main mechanism underlying the role of TRAP1 in tumor progression (24). Based on this rationale and since no evidence is at present available on TRAP1 function under oxygen deprivation conditions, at least to the best of our knowledge, the present study was designed to address the hypothesis that TRAP1 may be a key regulator of the CRC cell response to hypoxia.

Materials and methods

Cell cultures, reagents and cell transfection procedures. The HCT116 cell line (CCL-247) was purchased from the American Type Culture Collection (ATCC) and cultured in McCoy's 5A medium (cat. no. 26600023, Gibco; Thermo Fisher Scientific, Inc.), supplemented with 10% fetal bovine serum (cat. no. 10270106, Gibco; Thermo Fisher Scientific, Inc.), 1% glutamine (cat. no. 25030024, Gibco; Thermo Fisher Scientific, Inc.) and 1% penicillin and streptomycin (cat. N 15140122, Gibco; Thermo Fisher Scientific, Inc.). The 293T cell line (CRL-3216, ATCC) was cultured in Iscove's modified Dulbecco's medium (IMDM cat. no. 12440053, Gibco; Thermo Fisher Scientific, Inc.) supplemented with 10% heat-inactivated fetal calf serum (cat. no. S11450H, R&D Systems, Inc.), 1% glutamine (cat. no. 25030024, Gibco; Thermo Fisher Scientific, Inc.) and 1% penicillin and streptomycin (cat. no. 15140122, Gibco; Thermo Fisher Scientific, Inc.). The 293T cell line, characterized by high transfectability and transgenic expression, was used as a packaging cell line for generating viral particles. The authenticity of the cell lines was verified at the beginning of the study by STR profiling, in accordance with ATCC product description. Cell lines were routinely tested for mycoplasma contamination using the LookOut® Mycoplasma PCR Detection kit (cat. no. MP0035, MilliporeSigma). All cell lines were grown and maintained in a humidified incubator with 5% CO_2 and 95% (vol/vol) O_2. Hypoxic experiments were performed using the Galaxy 48-R incubator (New Brunswick Scientific Co., Inc.; Effendorf AG) at 0.5% O_2. HCT116 cells were also treated with hypoxia-mimic compound deferoxamine (cat. no. D9533, MilliporeSigma) at 250 μM for 6 h as a positive control of hypoxic experimental conditions.

TRAP1 transient silencing was performed using 80 nM siRNAs purchased from Qiagen (target sequence, 5'-CCCGGT CCCTGTACTCAGAAA-3'; sense strand, 5'-CGGUCCCUG UACUCAGAAATT-3'; antisense strand, 5'-UUUCUGAGU ACAGGGACCGGG-3'; cat. no. SI00115150, Qiagen GmbH). As a control, cells were transfected with the same amount of control siRNA (target sequence, N/A; sense and antisense sequence, proprietary; cat. no. SI03650318, Qiagen GmbH). Transient transfections of siRNAs were performed 48 h before the experiment using the HiPerFect Transfection Reagent (cat. no. 301705, Qiagen GmbH), according to the manufacturer's protocol.

mTOR inhibition in HCT116 cells was performed using everolimus (Afinitor, Novartis) at 1 μM for 24 h.

Glucose uptake and lactate production assays. Glucose uptake and lactate production were assessed as previously described (23). All experiments were performed at least in triplicate.

RNA extraction and reverse transcription-quantitative PCR (RT-qPCR). Total RNA was extracted using the RNeasy Plus Mini kit (cat. no. 74034, Qiagen GmbH), according to the manufacturer's instructions and reverse transcribed into cDNA using reverse transcription reagents (Superscript IV Vilo, cat. no. 11756050, Invitrogen; Thermo Fisher Scientific, Inc.), according to the manufacturer's instructions. qPCR analyses were performed in the CFX96 Touch™ Real-Time PCR Detection System (Bio-Rad Laboratories, Inc.) using SsoAdvanced™ Universal SYBR®-Green Supermix (cat. no. 1725271, Bio-Rad Laboratories, Inc.), according to the manufacturer's instructions. The reaction was conducted according to the following amplification protocol: 95˚C for 3 min, 39 cycles at 95˚C for 10 sec, 60˚C for 30 sec and 65-95˚C for 5 sec. Primers were purchased from MilliporeSigma or Invitrogen (Thermo Fisher Scientific, Inc.) and are listed in Table SI. Gene expression was analyzed according to $2^{-\Delta\Delta Cq}$ relative quantification method (26) using CFX Maestro software version 1.0 (Bio-Rad Laboratories, Inc.).

Western blot analysis. Cell pellets were lysed in ice-cold RIPA buffer [20 mmol/l Tris (pH 7.5) containing 300 mmol/l sucrose, 60 mmol/l KC1, 15 mmol/l NaC1, 5% (v/v) glycerol, 2 mmol/l EDTA, 1% (v/v) Triton X100, 1 mmol/l phenylmethylsulfonylfluoride, 2 mg/ml aprotinin, 2 mg/ml leupeptin and 0.2% (w/v) deoxycholate] as previously described (27). The protein concentration was measured using the Bio-Rad protein assay kit (cat. no. 5000006, Bio-Rad Laboratories, Inc.), according to the manufacturer's instructions. Samples were resolved by SDS-PAGE using polyacrylamide 4-20% precast gels (Mini-PROTEAN TGX Stain-Free Gels, cat. no. 4568094, Bio-Rad Laboratories, Inc.) and transferred onto a nitrocellulose membrane (Trans-Blot Turbo Transfer Pack, cat.

no. 1704158, Bio-Rad Laboratories, Inc.). The membrane was incubated for 60 min at room temperature with Western Blocker Solution (cat. no. W0138, MilliporeSigma) and immunoblotted with the following antibodies: Anti-TRAP1 (1:1,000 overnight 4˚C; cat. no. sc-73604, Santa Cruz Biotechnology, Inc.), anti-HIF-1α (1:2,000 overnight 4˚C; cat. no. ab16066, Abcam), anti-monocarboxylate transporter 4 (MCT4) (1:1,000 overnight 4˚C; cat. no. sc-376140, Santa Cruz Biotechnology, Inc.), anti-GLUT1 (1:1,000 overnight 4˚C; cat. no. ab32551, Abcam), anti-LDHA (1:1,000 overnight 4˚C; cat. no. sc-137243, Santa Cruz Biotechnology, Inc.), anti-p70S6 kinase α (H-9) (1:1,000 overnight 4˚C; cat. no. sc-8418, Santa Cruz Biotechnology, Inc.), anti-phospho-p70 S6 kinase (Thr389) (1:1,000 overnight 4˚C; cat. no. 9205, Cell Signaling Technology, Inc.) and β-actin (1:2,000 1 h room temperature; cat. no. sc-47778, Santa Cruz Biotechnology, Inc.). The expression of specific proteins was detected using a secondary antibody labeled with peroxidase 1:2,000 for 1 h room temperature [goat anti-mouse (H + L)-HRP conjugate, cat. no. 1706516, Bio-Rad Laboratories, Inc.; goat anti-rabbit (H + L)-HRP conjugate, cat. no. 1706515, Bio-Rad Laboratories, Inc.) and the Clarity Western ECL Substrate (cat. no. 1705061, Bio-Rad Laboratories, Inc.). Protein expression levels were quantified using densitometric analysis, using ImageJ software v1.53e (National Institutes of Health) and normalized according to the expression of housekeeping genes.

shTRAP1 p9T organoids. Human p9T CRC organoids were generated by the Jacco van Rheenen Research Group at the Department of Molecular Pathology of Netherlands Cancer Institute of Amsterdam (NKI-AVL) and kindly provided to the authors' laboratory. Organoids were cultured in a humidified atmosphere at 37˚C and 5% CO_2 with basal culture medium [Advanced DMEM/F12 (cat. no. 12634028, Gibco; Thermo Fisher Scientific, Inc.), 10 mM HEPES (cat. no. 15630056, Gibco; Thermo Fisher Scientific, Inc.), 2 mM Glutamax (cat. no. 35050061, Gibco; Thermo Fisher Scientific, Inc.), 100 U/ml penicillin and streptomycin (cat. no. 15140122, Gibco; Thermo Fisher Scientific, Inc.)] supplemented with 10% R-Spondin conditioned medium, 10% Noggin conditioned medium, 1X B27 (cat. no. 17504001, Gibco; Thermo Fisher Scientific, Inc.), 1.25 mM n-acetyl cysteine (cat. no. A9165, MilliporeSigma), 10 mM nicotinamide (cat. no. N0636, MilliporeSigma), 500 nM A83-01 (cat. no. SML0788, MilliporeSigma), 3 μM SB202190 (cat. no. CAY-10010399, Vinci-Biochem), 50 ng/ml human recombinant EGF (cat. no. 354052, BD Biosciences), 10 nM Leu15-Gastrin (cat. no. G9145, MilliporeSigma) and 10 nM prostaglandin E2 (cat. no. 14010, Vinci-Biochem). To confirm correct sample identity, the organoids were regularly tested by SNP analysis. Four different validated lentiviral reporter plasmids (pLKO.1_TRC cloning vector, plasmid#10878, Addgene, Inc.) for shTRAP1 were obtained from the NKI's Robotics and Screening Center Facility and tested to verify the silencing efficiency induced in CRC HCT116 cell line and organoids. Only two of these (shTRAP1#1 and shTRAP1#3) were selected for their high silencing efficiency and reduced mortality. The full hairpin sequences were as follows: shTRAP1#1, CCG GCCGCTACACCCTGCACTATAACTCGAGTTATAGTG CAGGGTGTAGCGGTTTTTG; and shTRAP1#3, CCGGCA GAGCACTCACCCTACTATGCTCGAGCATAGTAGGGT GAGTGCTCTGTTTTTG.

A 3rd generation lentiviral system was used, that includes pVSV-G (pMD2.G; plasmid #12259, Addgene, Inc.), pMDLg/pRRE (plasmid #12251, Addgene, Inc.) and pREV AmpR (pRSV-Rev; plasmid #12253, Addgene, Inc.) plasmids. The propagation of plasmids was performed in the bacterial strain DH5a into LB medium. DNA was isolated using the PureLink™ HiPure Plasmid Midiprep kit (cat. no. K210004, Invitrogen; Thermo Fisher Scientific, Inc.).

The 293T cells were transfected with the pLKO.1 vector coding for shTRAP1 using the calcium phosphate-DNA co-precipitation technique. The cell supernatant containing viral particles was collected, filtered and directly used for cell transduction, or ultracentrifuged (49,100 x g) for 2 h at 7˚C for organoid transduction. Lentiviral titers were determined using the qPCR Lentivirus Titration kit (LV900, Applied Biological Materials, Inc.), following the manufacturer's instructions. For the experiments, the amount of lentiviral supernatant used was calculated to achieve the multiplicity of infection (MOI) of 50. To ensure efficient transduction, the 293T and HCT116 cells were incubated with lentiviral supernatants at 37˚C for 24 h in the presence of polybrene (8 μg/ml, cat. no. TR-1003, MilliporeSigma). Antibiotic selection was initiated at 24 h post-transduction and was carried out for 5 consecutive days.

Tumor-derived p9T organoids were trypsinized using TrypLE (cat. no. 12605010, Gibco; Thermo Fisher Scientific, Inc.), mixed with 100 μl concentrated virus, 8 ng/ml polybrene and 10 μM Rho-associated, coiled-coil containing protein kinase inhibitor (Y-27632; cat. no. Y0503, MilliporeSigma) in 15 ml tubes and centrifuged at 600 x g for 1 h at 32˚C. Subsequently, the organoids were incubated at 37˚C and 5% CO_2 for 6 h. Following incubation, the organoids were washed with Advance DMEM/F12 medium and spun down for 5 min at 160 x g 4˚C to eliminate the virus. Following the removal of the virus-containing medium, organoids were plated in ~50 μl BME (cat. no. 353300502, Bio-Techne Corporation). Transduced organoids were grown in Advance DMEM/12 full of growth factors and fresh Y-27632 for 3 days after which selection was applied by the addition of puromycin (2 μg/ml, cat. no. A1113802, Thermo Fisher Scientific, Inc.) for 4 days.

Gene expression profiles. Total RNA (300 ng) was transcribed for the synthesis of cDNA and biotinylated cRNA, according to the protocol of the Illumina TotalPrep RNA (cat. no. AMIL1791, Ambion; Thermo Fisher Scientific, Inc.) amplification kit. The hybridization, marking and scanning of 750 ng cRNA was performed on the Illumina Human HT12 v4.0 Expression BeadChip array (Illumina Inc.), following the standard protocol. All analyses were performed in triplicate for each sample. The BeadChip was then dried and scanned using the Illumina HiScanHQ system (Illumina Inc.). Data analysis was carried out through the free/open source environment R/Bioconductor (28). Probes with a low quality of fluorescence intensity signal were excluded from the subsequent analysis steps. Normalization was performed using the neqc procedure, a background correction through internal controls followed by Quantile Normalization. The differential analysis between the experimental conditions and the normalization were performed using the limma package (29).

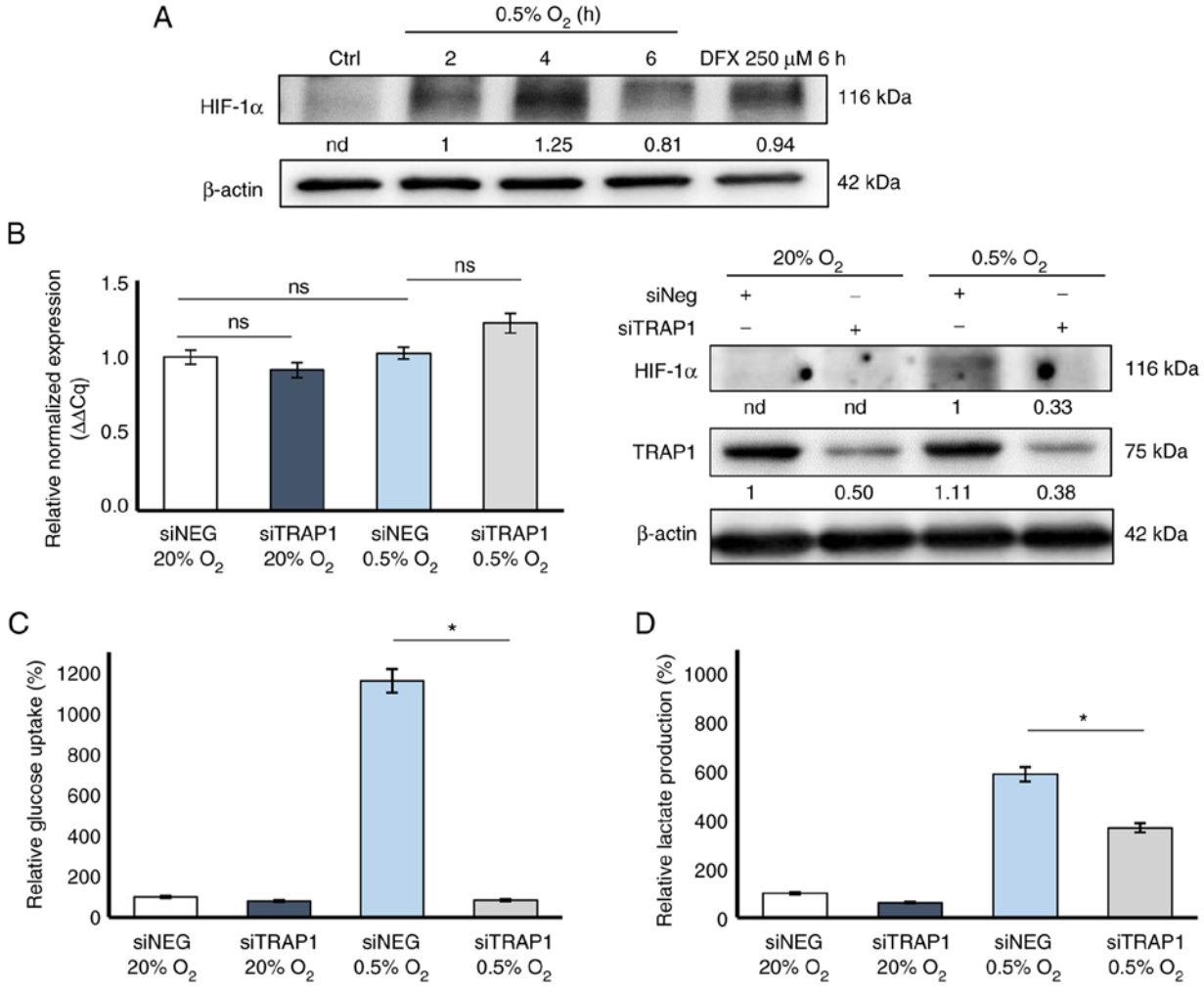

Figure 1. TRAP1 supports the hypoxia-induced metabolic rewiring of colorectal cancer cells via HIF-1α stabilization. (A) Western blot analysis of HIF-1α in HCT116 cells exposed to 20 (Ctrl) or 0.5% O_2 for 2, 4 and 6 h. Treatment with 250 μM deferoxamine (DFX) for 6 h was used as a positive control of HIF-1α stabilization. Densitometric analysis results are reported (nd, not detected). (B) Reverse transcription-quantitative PCR (left panel) and western blot analysis (right panel) analysis of HIF-1α expression in HCT116 cells transiently silenced or not for TRAP1 and exposed to hypoxia (0.5% O_2) or normoxia (20% O_2) for 4 h. (C) Relative glucose uptake and (D) lactate production in HCT116 cells transiently silenced or not for TRAP1 (siTRAP1) and exposed to hypoxia (0.5% O_2) or normoxia (20% O_2) for 4 h compared to the negative control (siNEG). P-values indicate statistically significant differences (*P<0.05). ns, not significant; TRAP1, TNF receptor-associated protein 1; HIF-1α, hypoxia inducible factor 1α.

Functional enrichment analysis was carried out through the Gene Set Enrichment Analysis (GSEA) (30) computational method and the MsigDB database (31) for the collection of annotated gene sets, focusing on the following categories: Hallmark, Gene Ontology and Pathways. The gene expression data generated in the present study have been deposited in the ArrayExpress database at EMBL-EBI (www.ebi.ac.uk/arrayexpress) under the accession no. E-MTAB-10563.

Analysis of public datasets. TRAP1 expression analysis in CRC samples, compared with normal tissue, was performed using the TNMplot database (https://www.tnmplot.com/). The platform directly compares tumor and normal samples and performs a Mann-Whitney U or Kruskal-Wallis tests or a paired Wilcoxon test (in case of availability of paired normal and adjacent tumor) for statistical significance (32).

Statistical analysis. The unpaired t-test was performed using the t-test Calculator of GraphPad (online version) for the analysis of metabolic tests in silenced cells and related controls (Fig. 1C and D). Data are reported as mean values of least three independent experiments (± SD). RT-qPCR data were analyzed using two-way ANOVA and Sidak's multiple comparisons test. Statistical analysis was performed using GraphPad 7.0 software (GraphPad Software, Inc.). A value of $P<0.05$ was considered to indicate a statistically significant difference.

Results

TRAP1 promotes hypoxia-induced metabolic rewiring in CRC cells via HIF-1α stabilization. In the preliminary analyses, TNMplot gene chip data were used to confirm the increased expression of TRAP1 in human CRC samples (n=160) compared to normal human colorectal mucosa (n=160). Notably, while the normal colorectal mucosa was characterized by a low TRAP1 mRNA expression, a significant upregulation of TRAP1 expression was observed in malignant tissues (Fig. S1A) ($P<0.001$ Kruskal-Wallis test). Considering that hypoxia is the main stimulus to boost glycolytic

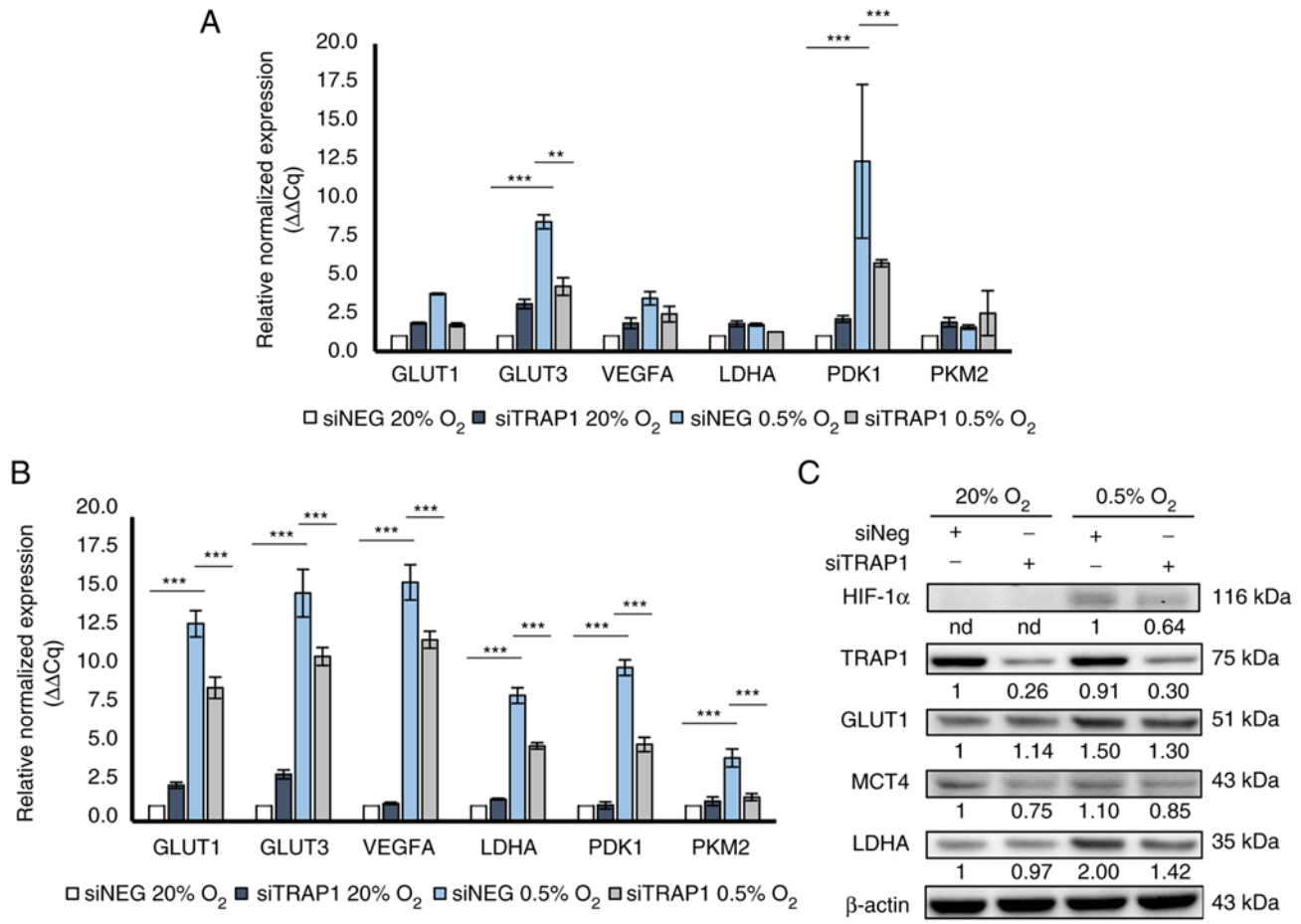

Figure 2. TRAP1 sustains HIF-1α-induced transcriptional reprogramming in HCT116 cells. (A and B) Reverse transcription-quantitative PCR analysis of metabolic HIF-1α inducible genes in HCT116 cells transiently silenced or not for TRAP1 and exposed to hypoxia (0.5% O_2) or normoxia (20% O_2) for (A) 8 h and (B) 24 h. P-values indicate statistically significant differences (**P<0.01 and ***P<0.001 comparing siNEG 0.5% O_2 vs. siNEG 20% O_2 and siTRAP1 0.5% O_2 vs. siNEG 0.5% O_2). (C) HIF-1α, TRAP1, GLUT1, MCT4 and LDHA western blot analysis in HCT116 cells transiently silenced or not for TRAP1 and exposed to hypoxia (0.5% O_2) or normoxia (20% O_2) for 24 h. Densitometric analysis results are reported (nd, not detected). TRAP1, TNF receptor-associated protein 1; HIF-1α, hypoxia inducible factor 1α; GLUT1, glucose transporter 1; MCT4, monocarboxylate transporter 4; LDHA, lactate dehydrogenase A.

metabolism in cancer cells (12,33-36), in order to establish the role of TRAP1 in hypoxia-induced metabolic rewiring, human CRC cells were used in the present study and in preliminary experiments; the optimal time for HCT116 cell exposure to 0.5% hypoxia to induce HIF-1α stabilization was evaluated. Western blot analysis revealed that HIF-1α maximal stabilization was observed after 4 h of exposure of the cells to 0.5% O_2 compared to normoxic conditions (20% O_2; Fig. 1A). In these experiments, HCT116 cells exposed to 250 μM deferoxamine for 6 h were used as a positive control.

To examine the role of TRAP1 in controlling HIF-1α stabilization in CRC, HCT116 cells were transiently silenced for TRAP1 and exposed to 4 h of hypoxia or normoxia and evaluated for HIF-1α stabilization using western blot analysis. Of note, although there were no significant differences in HIF-1α gene expression under the current experimental conditions (Fig. 1B, left panel), TRAP1 silencing induced a partial inhibition of HIF-1α stabilization at the post-translational level under hypoxic conditions (Fig. 1B, right panel).

In subsequent experiments, the association between TRAP1-mediated HIF-1α stabilization and its role in metabolic adaptive responses to reduced oxygen availability was investigated. Thus, TRAP1-silenced HCT116 cells were exposed to 0.5 and 20% O_2 for 4 h and analyzed for glucose uptake and lactate production. As was expected, hypoxia markedly enhanced both 2-DG uptake (Fig. 1C) and lactate production (Fig. 1D) in a high-TRAP1 background (siNEG). Of note, TRAP1 silencing significantly decreased 2-DG uptake (Fig. 1C) and partially impaired lactate production (Fig. 1D) under hypoxic conditions, thus suggesting that TRAP1 is required for hypoxia-induced metabolic rewiring.

TRAP1 sustains HIF-1α-induced transcriptional reprogramming in CRC cells and patient-derived organoids. To functionally characterize TRAP1-dependent HIF-1α stabilization in CRC, the role of TRAP1 in the HIF-1α-mediated transcriptional reprogramming of metabolic genes under hypoxic conditions was evaluated. HCT116 cells transiently silenced for TRAP1 were incubated for 8 and 24 h at 20 and 0.5% O_2 and assayed for the expression of both TRAP1 (Fig. S1B) and HIF-1α-inducible genes commonly involved in metabolic and angiogenic pathways (i.e., *GLUT1, GLUT3, VEGFA, LDHA, PDK1, PKM2*) (Fig. 2). Of note, TRAP1-silenced HCT116 cells failed to significantly activate the expression of some of the evaluated genes after 8 h of hypoxia compared to the control cells; the differential expression of GLUT3 (P<0.01)

and PDK1 (P<0.001) was statistically significant (Fig. 2A). Consistently, TRAP1 silencing resulted in the reduced expression of all tested genes under 24 h of hypoxia (P<0.001; Fig. 2B). Under normoxic conditions, no significant differences were observed between the TRAP1-silenced and control cells at all time points, with similar expression levels observed for all tested genes (Fig. 2A and B). In parallel experiments, western blot analysis was used to evaluate HIF-1α stabilization and the expression of certain HIF-1α-target genes, i.e., GLUT1, LDHA and MCT4 in a high vs. low TRAP1 background under hypoxic conditions (Fig. 2C). Consistent with the RT-qPCR data, TRAP1 silencing led to the lower stabilization of HIF-1α and to lower levels of GLUT1, LDHA and MCT4 under hypoxic conditions compared to the control cells.

These experiments were further extended to a 3D-model of human CRC organoids, based on the rationale that the growth of organoids within a 3D matrix favors the spontaneous generation of hypoxic areas, as observed in tumors (37). For these experiments, pMOCK and TRAP1-silenced p9T organoids were generated. Four different shTRAP1 lentiviruses (#1, #2, #3 and #4) were first tested for the efficiency of transfection in both 293T and HCT116 cells evaluating TRAP1 silencing using RT-qPCR and western blot analysis (Fig. S1C, left and right panels, respectively), and shTRAP1 #1 and shTRAP1 #3 lentiviruses were selected for their highest silencing effectiveness. In subsequent experiments, shTRAP1 #1 and shTRAP1 #3 were tested for the efficiency of transduction in p9T organoids (Fig. S1D) and shTRAP1 #1 p9T organoids were used for further experiments aimed at validating the role of TRAP1 in the regulation of HIF-1α transcriptional activity. pMOCK and TRAP1-silenced p9T organoids were incubated for 8 and 24 h at 0.5 and 20% O_2 and analyzed using RT-qPCR for TRAP1 (Fig. S1E) and HIF-1α inducible genes (Fig. 3) expression levels. The majority of genes exhibited a significant and progressive upregulation in a TRAP1 high expression background under hypoxic conditions starting from 8 h (Fig. 3A) and reaching the highest level at 24 h (Fig. 3B). Notably, TRAP1 silencing resulted in a decreased expression of all tested genes under hypoxic conditions (Fig. 3), with maximal statistical significance at 24 h, as observed in the HCT116 cells.

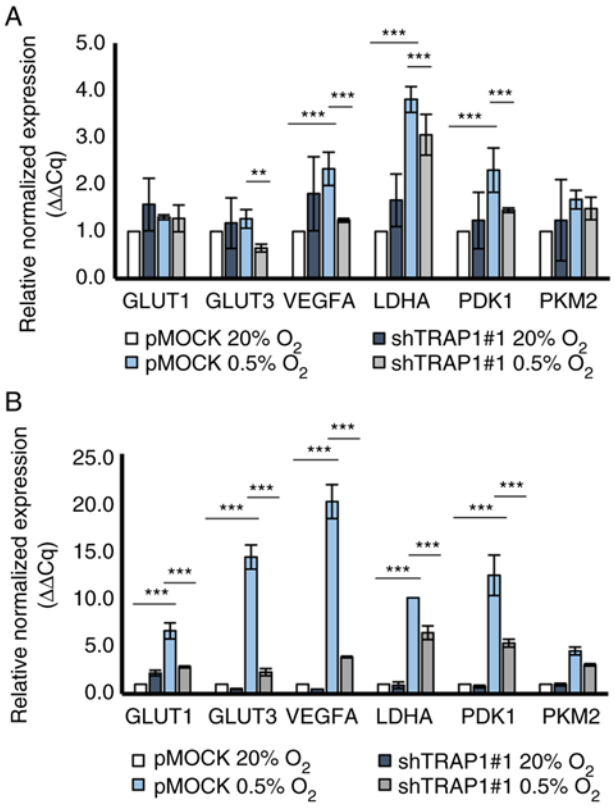

Figure 3. TRAP1 sustains HIF-1α-induced transcriptional activity in human CRC organoids. (A and B) Reverse transcription-quantitative PCR analysis of metabolic HIF-1α inducible genes in shTRAP1#1 p9T organoids exposed to hypoxia (0.5% O_2) or normoxia (20% O_2) for (A) 8 h and (B) 24 h. P-values indicate statistically significant differences (**P<0.01 and ***P<0.001 by comparing pMOCK 0.5% O_2 vs. pMOCK 20% O_2 and shTRAP1#1 0.5% O_2 vs. pMOCK 0.5% O_2). TRAP1, TNF receptor-associated protein 1; HIF-1α, hypoxia inducible factor 1α.

TRAP1 silencing promotes ribosomal biogenesis under hypoxic conditions. As data described above demonstrating a role of TRAP1 in hypoxia-induced gene expression reprogramming, a whole genome gene expression profiling was performed in TRAP1-silenced and control HCT116 cells exposed to normoxia and hypoxia for 24 h. As was expected, oxygen deprivation promoted significant gene expression reprogramming with 2,665 downregulated and 2,041 upregulated genes compared to the normoxic control (abs logFC ≥0.60, P<0.05). Furthermore, 1,071 genes were differentially expressed (347 downregulated and 724 upregulated) in TRAP1-silenced compared to control HCT116 cells under hypoxic conditions (abs logFC ≥0.60, P<0.05) (Table SII).

GSEA was performed to obtain functional enrichments of differentially expressed genes focusing on the following categories: Hallmark, Gene Ontology (GO) and Pathway (abs enrichment score ≥0.60, P<0.05) (Table SIII). Although very few Hallmarks were enriched, the two most upregulated Hallmarks under hypoxic conditions were HYPOXIA and ANGIOGENESIS, confirming that, under the current experimental conditions, hypoxic stress regulated gene expression to promote oncogenic and angiogenetic pathways (10-16). Furthermore, several GOs and Pathways were functionally regulated in our experimental conditions. In particular, 453 (227 downregulated and 226 upregulated) and 201 (62 downregulated and 139 upregulated) GOs were enriched comparing hypoxia (siNEG 0.5% O_2) vs. normoxia (siNEG 20% O_2) and a low vs. high TRAP1 background under hypoxic conditions (siTRAP1 0.5% O_2 vs. siNEG 0.5% O_2), respectively. Among these, 58 enriched GOs were present in both datasets and most of these exhibited an opposite regulation after TRAP1 silencing under hypoxic conditions, being up/downregulated in response to hypoxia in a high TRAP1 background and down/upregulated upon TRAP1 silencing under hypoxic conditions (Table SIV).

Focusing on the top five more significantly enriched GOs in siTRAP1 0.5% O_2 vs. siNEG 0.5% O_2, a positive regulation of ribosomal small subunit biogenesis emerged, including the co-transcriptional assembly of tricistronic pre-rRNA into the small subunit (SSU) processome and the subsequent maturation of SSU rRNA 18S, contained in the 40S subunit of the mature ribosome (Fig. 4A). Noteworthy, these GOs were negatively regulated by hypoxia and their downregulation was prevented by TRAP1 silencing under hypoxic conditions.

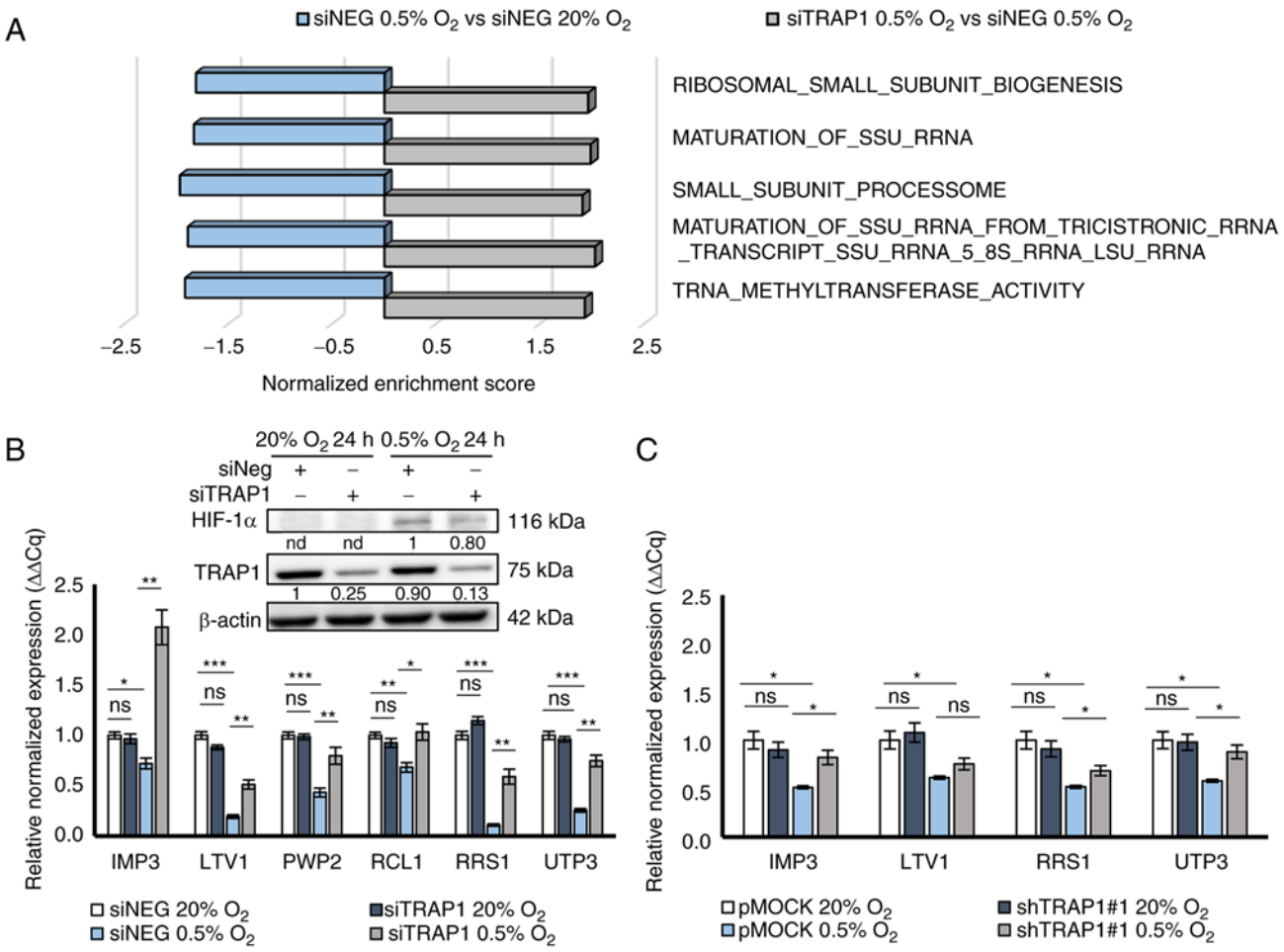

Figure 4. TRAP1 silencing promotes the ribosomal biogenesis under hypoxic conditions. (A) Top five most significantly enriched Gene Ontology terms upregulated comparing siTRAP1 0.5% O_2 vs. siNEG 0.5% O_2 and downregulated in siNEG 0.5% O_2 vs. siNEG 20% O_2 (abs ES >0.60; P<0.01). (B and C) Reverse transcription-quantitative PCR analysis of ribosome biogenesis-related genes in (B) TRAP1-silenced HCT116 cells exposed to hypoxia (0.5% O_2) or normoxia (20% O_2) for 24 h and (C) shTRAP1#1 p9T organoids exposed to hypoxia (0.5% O_2) or normoxia (20% O_2) for 8 h. P-values indicate statistically significant differences (*P<0.05, **P<0.01 and ***P<0.001). (B) Insert: TRAP1 and HIF-1α western blot analysis in TRAP1-silenced HCT116 cells exposed to hypoxia (0.5% O_2) or normoxia (20% O_2) for 24 h. TRAP1, TNF receptor-associated protein 1; HIF-1α, hypoxia inducible factor 1α.

Instead, none of these GOs was enriched following TRAP1 silencing under normoxic conditions (siTRAP1 20% O_2 vs. siNEG 20% O_2).

To validate the possible role of TRAP1 in sustaining the ribosome biogenesis inhibition under hypoxic conditions, six genes were selected (i.e., *IMP3, LTV1, PWP2, RCL1, RRS1* and *UTP3*) commonly involved in different steps of ribosome biogenesis and maturation and differentially expressed in the current experimental conditions, thus contributing to the enrichment of previous GO categories (abs logFC ≥0.60, P<0.05). The expression levels of these genes were evaluated using RT-qPCR in both HCT116 cells and p9T organoids silenced or not for TRAP1 and exposed to hypoxia for 24 and 8 h, respectively (Fig. 4B and C). These time points were selected based on data reported in Figs. 2 and 3, demonstrating an earlier transcriptional reprogramming in response to hypoxia in CRC organoids. No difference in expression was observed for all tested genes in TRAP1-silenced cells (Fig. 4B) and shTRAP1#1 p9T organoids (Fig. 4C) compared to controls under normoxic conditions; this was consistent with the GSEA data demonstrating no enrichment of ribosome biogenesis/assembly GO categories under normoxic conditions. Conversely, as was expected, the hypoxic stimulus significantly suppressed the expression of these genes in both the CRC experimental models and TRAP1 silencing attenuated the inhibitory effects of hypoxia by promoting a higher expression of these genes under hypoxic conditions (Fig. 4B and C). Two genes (i.e., PWP2 and RCL1) were undetectable in p9T organoids and, thus, are not illustrated in Fig. 4.

mTOR pathway is likely involved in the TRAP1 regulation of ribosome biogenesis. Based on the hypothesis that the TRAP1 modulation of ribosome biogenesis under hypoxic conditions may involve the mTORC1/p70S6K pathway, western blot analysis was performed to evaluate the phosphorylation status of p70S6K, a master regulator of protein synthesis and ribosome biogenesis, in TRAP1-silenced HCT116 cells exposed to hypoxia and treated with the mTOR inhibitor everolimus at 1 μM for 24 h (Fig. 5A). Unlike oxygen deprivation that suppressed p70S6K phosphorylation, TRAP1 silencing enhanced p70S6K activation/phosphorylation compared to the respective controls and this occurred both under normoxic and hypoxic conditions. Moreover, the mTOR inhibitor, everolimus,

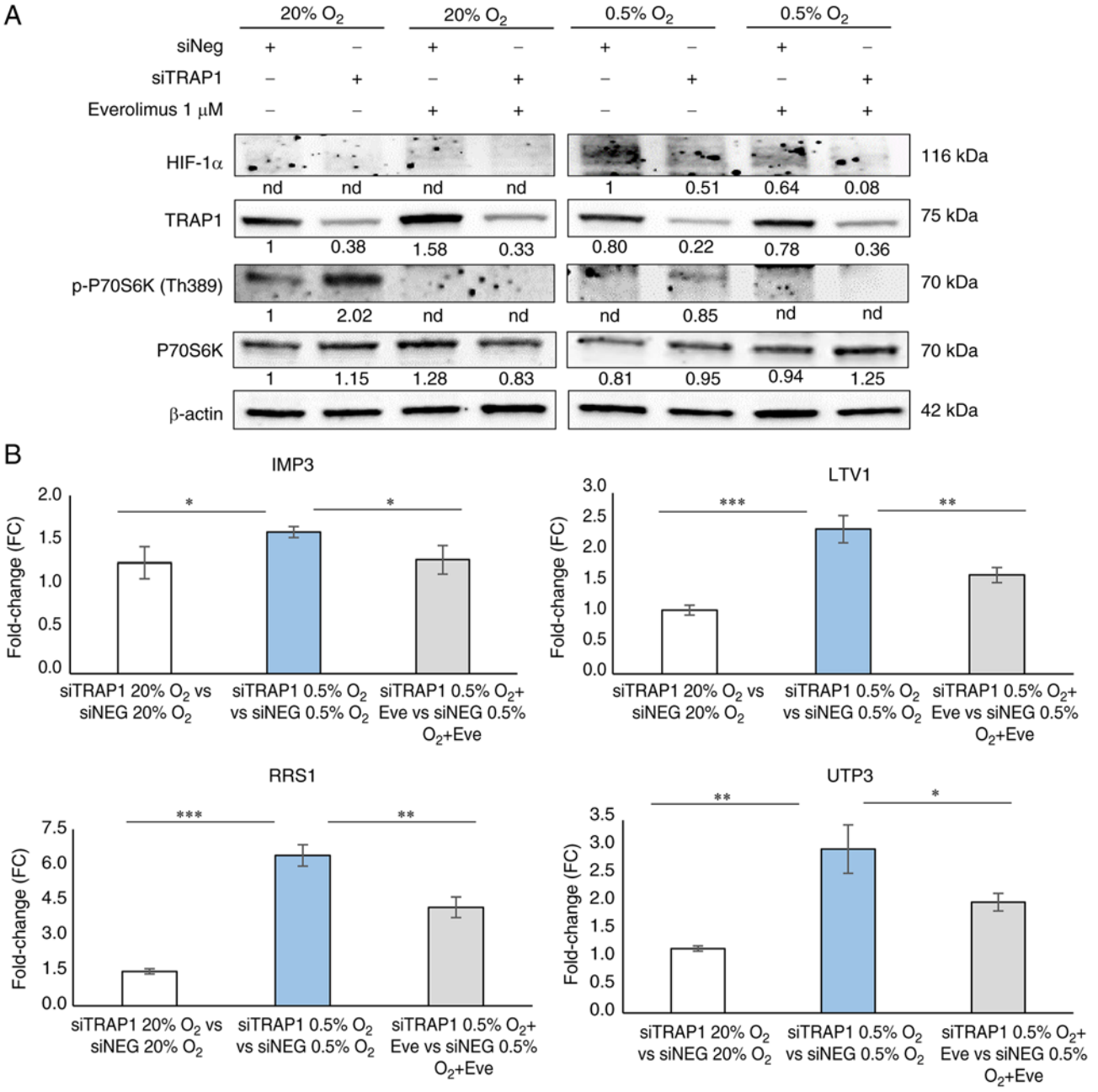

Figure 5. TRAP1 regulation of ribosome biosynthesis occurs through mTOR signaling regulation. (A) HIF-1α, P70S6K and p-P70S6K western blot analysis in TRAP1-silenced HCT116 cells exposed to hypoxia (0.5% O_2) or normoxia (20% O_2) for 24 h in the presence or absence of 1 μM everolimus. Densitometric analysis results are reported (nd, not detected). (B) Reverse transcription-quantitative PCR analysis of ribosome biogenesis-related genes in TRAP1-silenced HCT116 cells exposed to hypoxia (0.5% O_2) or normoxia (20% O_2) for 24 h in the presence or absence of 1 μM everolimus. Data are expressed as the FC increase of gene expression in TRAP1-silenced cells compared to the respective control under normoxic or hypoxic conditions and in the presence or absence of everolimus. Statistically significant differences among FC values are indicated as *P<0.05, **P<0.01 and ***P<0.001. FC, fold change; TRAP1, TNF receptor-associated protein 1; HIF-1α, hypoxia inducible factor 1α.

hampered p70S6K phosphorylation under normoxic and hypoxic conditions, and in high and low TRAP1 expression backgrounds (Fig. 5A).

To corroborate the link between the TRAP1 regulation of the mTOR pathway and its control of ribosome biogenesis under hypoxic conditions, four ribosome biogenesis-related genes (i.e., *IMP3, LTV1, RRS1* and *UTP3*) were further evaluated using RT-qPCR in TRAP1-silenced cells exposed to normoxia and hypoxia for 24 h in the presence or absence of everolimus (Fig. 5B). Data are reported as the fold change (FC) increase in gene expression in TRAP1-silenced cells compared to the respective control under normoxic and hypoxic conditions, and in the presence or absence of everolimus. As observed in Fig. 4A, TRAP1 silencing resulted in the upregulation of the expression of these genes under hypoxic conditions, and this occurred in parallel with mTOR signaling activation (Fig. 5A). Of note, mTOR signaling inhibition by everolimus in TRAP1-silenced cells attenuated the upregulation of these genes (Fig. 5B). According to previously described data, no significant differences (FC <1.5) were observed after TRAP1 silencing under normoxic conditions (siTRAP1 20% O_2 vs. siNEG 20% O_2).

Discussion

CRC is responsible for 10% of all cancer types, affecting almost 1.9 million new individuals each year (38) and its mortality rate results in almost 880,000 deaths/year, rendering CRC the second-leading cause of cancer-related deaths (39,40). Despite important advancements in CRC therapy, the vast majority of patients with metastatic disease experience disease progression in response to current treatments and thus, the identification of novel reliable biomarkers and/or targetable pathways associated with CRC onset and progression is required. In this context, metabolic pathways are currently regarded as novel therapeutic targets in solid tumors (41,42), based on the rationale that metabolic reprogramming is considered a hallmark of cancer and supports cancer cell growth and proliferation as well as cell adaptation to unfavorable microenvironments (43).

A frequent stressful condition for solid tumors is the limited availability of oxygen, to which cancer cells can rapidly adapt by activating several survival pathways and, among others, stabilizing the transcription factor HIF-1α, which plays a fundamental role in mediating cellular adaptive responses, inducing the expression of several metabolic genes (11-15) and inhibiting high energy consuming processes (44-47). Indeed, HIF-1α is widely considered the master regulator of cancer cell response to oxygen deprivation and its activation favors a rapid and sustained reprogramming of cancer cells, leading to the induction of angiogenesis and metabolic rewiring towards Warburg metabolism (10,16).

Molecular chaperones function as hub proteins connecting metabolic pathways and cancer cell reprogramming mechanisms (22,48). The authors have previously reported that TRAP1 is upregulated in human CRCs (18,49) and that its expression is directly associated with a poor clinical outcome (18), drug resistance (49) and the inhibition of mitochondrial respiration (24). Recently, it emerged that high TRAP1 levels enhance Warburg metabolism in CRC tissues, patient-derived spheroids and cell lines and that this molecular chaperone can modulate glycolysis controlling PFK1 activity/stability (23). Furthermore, it has already been reported that TRAP1 is involved in HIF-1α stabilization under normoxic conditions and that this process occurs downstream of TRAP1 inhibition of succinate dehydrogenase and respiratory chain (24). Indeed, TRAP1 inhibits complexes II and IV of the respiratory chain with consequent succinate accumulation and favors HIF-1α stabilization due to inhibition of prolyl hydrolases and HIF-1α degradation (24,25).

In the present study, the role of TRAP1 in controlling cell response to hypoxia was investigated in CRC cell models, using both stabilized cell lines and organoids. It was observed that TRAP1 supports hypoxia-induced metabolic rewiring, increases glucose intake and lactate production and supports HIF-1α stabilization under hypoxia, thus favoring cellular adaptation to oxygen deprivation. Furthermore, TRAP1-mediated HIF-1α stabilization functionally sustains HIF-1α-dependent gene expression reprogramming in both human CRC cells and patient-derived organoids. Thus, it can be hypothesized that TRAP1 is responsible for HIF-1α stabilization under either hypoxic or normoxic conditions, and that this is likely finalized to reprogram tumor metabolism and sustain the oncogenic program induced by hypoxia.

In a translational perspective, it is important to underline that these observations were not only reproduced, but also more evident in CRC organoids, a tridimensional tumor model that resembles several characteristics of human solid tumors (50-52). In particular, the data of the present study demonstrated an earlier transcriptional reprogramming in response to hypoxia in organoids compared to monolayer cells, since their growth within a 3D matrix already promotes the formation of spontaneous hypoxic area which characterize solid tumors (37). 2D cell cultures cannot reproduce the spatial oxygen gradient and spatial heterogeneity observed *in vivo* in tumors (53), as cancer cells are exposed to a fixed concentration of oxygen partial pressure. Therefore, it is not surprising that the 3D organoid model has often recently been used to mimic hypoxic conditions and *in vivo* intratumoral heterogeneity (54). Furthermore, the present study suggested that a low TRAP1 expression background induced a greater inhibitory effect on HIF-1α target gene expression under hypoxic conditions in p9T organoids compared to HCT116 cells, and this can be explained by the different cell system and the higher efficacy and stability of shRNA silencing by lentiviral transduction technology.

The adaptive response to hypoxic stress also involves the inhibition of high-energy consuming processes as ribosome biogenesis and protein synthesis (44-47). Indeed, hypoxia induces the inhibition of the mTORC1 kinase (47,55-57), a master regulator of cellular growth and proliferation and mRNA translation (58,59). mTORC1 is a conserved serine/threonine kinase that phosphorylates downstream substrates involved in protein synthesis as eukaryotic initiation factor 4E (eIF4E)-binding protein 1 (4E-BP1) and ribosomal protein kinase S6 (S6K1 or p70S6K) (60). The activation of mTORC1 stimulates protein synthesis and cell growth by targeting effectors of both translation efficiency by existing ribosomes and synthesis of new ribosomes (61). In particular, mTORC1 coordinates the synthesis of ribosomal RNA (rRNA) and ribosomal proteins, the major constituents of the ribosome (62-66). Indeed, mTORC1/p70S6K signaling is required for the translation of mRNAs with 5'-terminal oligopyrimidine tract (5'-TOP) sequences, among which many encode for ribosomal proteins or regulators of translation (67-70). Additionally, p70S6K indirectly enhances the transcription of the 45S ribosomal gene (rDNA) that encodes for 18S, 28S and 5.8S rRNAs (63). In the present study, gene expression analysis performed under hypoxic conditions and in a low vs. high TRAP1 expression background, suggests that ribosome biosynthesis is a main process downregulated in response to oxygen deprivation and this requires high TRAP1 expression. This observation is consistent with the findings of other studies suggesting that TRAP1 influences adaptive biosynthetic processes responsible for the optimization of cancer cell response to stress (71), with TRAP1 being responsible for the cell response to endoplasmic reticulum stress (72), the quality control of mitochondria-destined proteins (73) and the attenuation of protein synthesis (70). Furthermore, previous research by the authors has demonstrated a role of TRAP1 in regulating p70S6K phosphorylation and the cap-mediated translation pathway in cancer cells (74). Thus, it can be hypothesized that TRAP1 is at the crossroads between the HIF-1α and mTORC1 pathways, both involved in cell responses to environmental

stress conditions. HIF-1α is responsible for mTORC1 inhibition (47,55-57) and as mTORC1 signaling is a key regulator of ribosome biogenesis and protein synthesis (60-70), taken together, these data suggest that this network is finalized at optimizing metabolic and biosynthetic processes in cancer cells under conditions of oxygen deprivation, thus, favoring the adaptation to a condition of substrates and energy restriction. Of note, the upregulation of such a network in cancer cells may provide survival and adaptive mechanisms that sustain cancer progression in a hostile environment. However, it is important to underline that these data do not fully demonstrate the mechanistic link between HIF-1α stabilization, mTORC1 inhibition and ribosome biogenesis downregulation in a high TRAP1 expression background; thus, further studies are required to depict the mechanisms involved at the molecular level.

The findings of the present study support the hypothesis that the intricate process of ribosomal subunits synthesis and maturation is controlled by the TRAP1/HIF-1α/mTORC1 network at multiple steps. In this context, TRAP1 pathways indirectly control the expression of several genes (i.e., *PWP2, IMP3, UTP3, RCL1, LTV1* and *RRS1*) coding for proteins playing a role in different steps of ribosome production (75-85). Their expression is downregulated in parallel with mTORC1 inhibition under hypoxic conditions in a high TRAP1 expression background, it is preserved upon TRAP1 silencing under oxygen deprivation conditions, and it is downregulated upon mTOR inhibition in a low TRAP1 expression background. Taken together, these data suggest that the TRAP1 regulation of ribosome biosynthesis under hypoxic conditions occurs through mTORC1 signaling regulation and that this involves the modulation of multiple enzymes.

In conclusion, the results of the present study support a role of TRAP1 in favoring human CRC adaptive responses to oxygen deprivation. Indeed, TRAP1 i) controls HIF-1α stabilization and maximizes Warburg metabolism in response to hypoxia; ii) is able to sustain the oncogenic program induced by hypoxia; and iii) modulates ribosome biogenesis in response to hypoxia to limit cellular energy consumption and this occurs through the mTOR pathway inhibition. Thus, TRAP1 may be considered a potential target for developing innovative therapies aimed at blocking molecular mechanisms that allow cancer cells to survive to unfavorable environmental conditions.

Acknowledgements

The authors would like to thank the research group of Professor Jacco van Rheenen for their cooperation with the generation of organoids, using samples from NKI-AVL Biobank.

Funding

The present study was supported by the '5 per mille' 2018-2019 LILT Investigator Grant. The present study was also supported by PON AIM R&I 2014-2020-1879351-2. This manuscript has been published with the financial support of the Department of Medical and Surgical Sciences of the University of Foggia (project code FINATENEO_DIRETTORE_ASSNEQUALITA_MEDCHIR_2021) and the University of Foggia (Fondo per i Progetti di Ricerca di Ateneo-PRA 2020).

Availability of data and materials

All data generated or analyzed during this study are included in this published article (and in the supplementary files).

Author's contributions

ML conceived the study and designed the experiments. VLB performed the metabolic experiments and generated the TRAP1-silenced organoids in collaboration with the research group of Professor Jacco van Rheenen (mentioned above). GB and VLB performed the RT-qPCR analysis. VLB and AP performed the western blot analysis. FC, VC and MP performed the whole genome gene expression profiling. PZ, GB and AP analyzed the whole genome gene expression profiling data. FM contributed to the metabolic experiments. GG, DSM and FE assisted in the design of the experiments and in the analysis of the data. GB and ML wrote the manuscript with the assistance of GG, DSM and FE. All authors have read and approved the final manuscript. GB, VLB, VC and PZ confirm the authenticity of all the raw data.

Ethics approval and consent to participate

Organoids were generated by the Nederlands Kanker Instituut-Antoni van Leeuwenhoek (NKI-AVL) and provided to the authors' laboratory according to an MTA for Academic Institutions. Organoids were generated in accordance with all applicable Nederland laws and regulations, including but not limited to patient's informed consent and in accordance with the NKI-AVL Institutional Review Board procedure, and the approval of the Medical Ethical Committee (MEC) of the NKI-AVL. Thus, according to the MTA, the organoids were used only for research scopes following the NKI-AVL institutional indications.

Patient consent for publication

Not applicable.

Competing interests

The authors declare that they have no competing interests.

References

1. Vander Heiden MG and DeBerardinis RJ: Understanding the intersections between metabolism and cancer biology. Cell 168: 657-669, 2017.
2. Liberti MV and Locasale JW: The Warburg effect: How does it benefit cancer cells? Trends Biochem Sci 41: 211-218, 2016.
3. Schwartz L, Supuran CT and Alfarouk KO: The Warburg effect and the hallmarks of cancer. Anticancer Agents Med Chem 17: 164-170, 2017.
4. Yu L, Lu M, Jia D, Ma J, Ben-Jacob E, Levine H, Kaipparettu BA and Onuchic JN: Modeling the genetic regulation of cancer metabolism: Interplay between glycolysis and oxidative phosphorylation. Cancer Res 77: 1564-1574, 2017.
5. Jing X, Yang F, Shao C, Wei K, Xie M, Shen H and Shu Y: Role of hypoxia in cancer therapy by regulating the tumor microenvironment. Mol Cancer 18: 157, 2019.
6. Zhang Y, Zhang H, Wang M, Schmid T, Xin Z, Kozhuharova L, Yu WK, Huang Y, Cai F and Biskup E: Hypoxia in breast cancer-scientific translation to therapeutic and diagnostic clinical applications. Front Oncol 11: 652266, 2021.

7. Miranda E, Nordgren IK, Male AL, Lawrence CE, Hoakwie F, Cuda F, Court W, Fox KR, Townsend PA, Packham GK, *et al*: A cyclic peptide inhibitor of HIF-1 heterodimerization that inhibits hypoxia signaling in cancer cells. J Am Chem Soc 135: 10418-10425, 2013.
8. Burslem GM, Kyle HF, Nelson A, Edwards TA and Wilson AJ: Hypoxia inducible factor (HIF) as a model for studying inhibition of protein-protein interactions. Chem Sci 8: 4188-4202, 2017.
9. Nagao A, Kobayashi M, Koyasu S, Chow CCT and Harada H: HIF-1-dependent reprogramming of glucose metabolic pathway of cancer cells and its therapeutic significance. Int J Mol Sci 20: 238, 2019.
10. Saponaro C, Malfettone A, Ranieri G, Danza K, Simone G, Paradiso A and Mangia A: VEGF, HIF-1α expression and MVD as an angiogenic network in familial breast cancer. PLoS One 8: e53070, 2013.
11. Shen LF, Zhou SH and Yu Q: Relationships between expression of glucose transporter protein-1 and hypoxia inducible factor-1α, prognosis and ^{18}F-FDG uptake in laryngeal and hypopharyngeal carcinomas. Transl Cancer Res 9: 2824-2837, 2020.
12. Semenza GL: HIF-1 mediates metabolic responses to intratumoral hypoxia and oncogenic mutations. J Clin Invest 123: 3664-3671, 2013.
13. He G, Yi J, Bo Z and Wu G: The effect of HIF-1α on glucose metabolism, growth and apoptosis of pancreatic cancerous cells. Asia Pac J Clin Nutr 23: 174-180, 2014.
14. Goodwin J, Choi H, Hsieh MH, Neugent ML, Ahn JM, Hayenga HN, Singh PK, Shackelford DB, Lee IK, Shulaev V, *et al*: Targeting hypoxia-inducible factor-1α/pyruvate dehydrogenase kinase 1 axis by dichloroacetate suppresses bleomycin-induced pulmonary fibrosis. Am J Respir Cell Mol Biol 58: 216-231, 2018.
15. Kierans SJ and Taylor CT: Regulation of glycolysis by the hypoxia-inducible factor (HIF): Implications for cellular physiology. J Physiol 599: 23-37, 2021.
16. Samec M, Liskova A, Koklesova L, Mersakova S, Strnadel J, Kajo K, Pec M, Zhai K, Smejkal K, Mirzaei S, *et al*: Flavonoids targeting HIF-1: Implications on cancer metabolism. Cancers (Basel) 13: 130, 2021.
17. Condelli V, Crispo F, Pietrafesa M, Lettini G, Matassa DS, Esposito F, Landriscina M and Maddalena F: HSP90 molecular chaperones, metabolic rewiring, and epigenetics: Impact on tumor progression and perspective for anticancer therapy. Cells 8: 532, 2019.
18. Maddalena F, Simeon V, Vita G, Bochicchio A, Possidente L, Sisinni L, Lettini G, Condelli V, Matassa DS, Li Bergolis V, *et al*: TRAP1 protein signature predicts outcome in human metastatic colorectal carcinoma. Oncotarget 8: 21229-21240, 2017.
19. Amoroso MR, Matassa DS, Sisinni L, Lettini G, Landriscina M and Esposito F: TRAP1 revisited: Novel localizations and functions of a 'next-generation' biomarker (review). Int J Oncol 45: 969-977, 2014.
20. Masgras I, Sanchez-Martin C, Colombo G and Rasola A: The chaperone TRAP1 as a modulator of the mitochondrial adaptations in cancer cells. Front Oncol 7: 58, 2017.
21. Avolio R, Matassa DS Criscuolo D, Landriscina M and Esposito F: Modulation of mitochondrial metabolic reprogramming and oxidative stress to overcome Chemoresistance in Cancer. Biomolecules 10: 135, 2020.
22. Matassa DS, Agliarulo I, Avolio R, Landriscina M and Esposito F: TRAP1 regulation of cancer metabolism: Dual role as oncogene or tumor suppressor. Genes (Basel) 9: 195, 2018.
23. Maddalena F, Condelli V, Matassa DS, Pacelli C, Scrima R, Lettini G, Li Bergolis V, Pietrafesa M, Crispo F, Piscazzi A, *et al*: TRAP1 enhances Warburg metabolism through modulation of PFK1 expression/activity and favors resistance to EGFR inhibitors in human colorectal carcinomas. Mol Oncol 14: 3030-3047, 2020.
24. Sciacovelli M, Guzzo G, Morello V, Frezza C, Zheng L, Nannini N, Calabrese F, Laudiero G, Esposito F, Landriscina M, *et al*: The mitochondrial chaperone TRAP1 promotes neoplastic growth by inhibiting succinate dehydrogenase. Cell Metab 17: 988-999, 2013.
25. Yoshida S, Tsutsumi S, Muhlebach G, Sourbier C, Lee MJ, Lee S, Vartholomaiou E, Tatokoro M, Beebe K, Miyajima N, *et al*: Molecular chaperone TRAP1 regulates a metabolic switch between mitochondrial respiration and aerobic glycolysis. Proc Natl Acad Sci USA 110: E1604-E1612, 2013.
26. Livak KJ and Schmittgen TD: Analysis of relative gene expression data using real-time quantitative PCR and the 2(-Delta Delta C(T)) method. Methods 25: 402-408, 2001.
27. Landriscina M, Laudiero G, Maddalena F, Amoroso MR, Piscazzi A, Cozzolino F, Monti M, Garbi C, Fersini A, Pucci P and Esposito F: Mitochondrial chaperone Trap1 and the calcium binding protein Sorcin interact and protect cells against apoptosis induced by antiblastic agents. Cancer Res 70: 6577-6586, 2010.
28. R Core Team: R: A language and environment for statistical computing. R Foundation for Statistical Computing, Vienna, 2019. https://www.R-project.org/.
29. Ritchie ME, Phipson B, Wu D, Hu Y, Law CW, Shi W and Smyth GK: limma powers differential expression analyses for RNA-sequencing and microarray studies. Nucleic Acids Res 43: e47, 2015.
30. Zito A, Lualdi M, Granata P, Cocciadiferro D, Novelli A, Alberio T, Casalone R and Fasano M: Gene set enrichment analysis of interaction networks weighted by node centrality. Front Genet 12: 577623, 2021.
31. Liberzon A, Birger C, Thorvaldsdóttir H, Ghandi M, Mesirov JP and Tamayo P: The molecular signatures database (MSigDB) hallmark gene set collection. Cell Syst 1: 417-425, 2015.
32. Bartha Á and Győrffy B: TNMplot.com: A web tool for the comparison of gene expression in normal, tumor and metastatic tissues. Int J Mol Sci 22: 2622, 2021.
33. Grandjean G, de Jong PR, James B, Koh MY, Lemos R, Kingston J, Aleshin A, Bankston LA, Miller CP, Cho EJ, *et al*: Definition of a novel feed-forward mechanism for glycolysis-HIF1α signaling in hypoxic tumors highlights aldolase A as a therapeutic target. Cancer Res 76: 4259-4269, 2016.
34. Xie H and Simon MC: Oxygen availability and metabolic reprogramming in cancer. J Biol Chem 292: 16825-16832, 2017.
35. Nowak N, Kulma A and Gutowicz J: Up-regulation of key glycolysis proteins in cancer development. Open Life Sci 13: 569-581, 2018.
36. Hao X, Ren Y, Feng M, Wang Q and Wang Y: Metabolic reprogramming due to hypoxia in pancreatic cancer: Implications for tumor formation, immunity, and more. Biomed Pharmacother 141: 111798, 2021.
37. Silva-Almeida C, Ewart MA and Wilde C: 3D gastrointestinal models and organoids to study metabolism in human colon cancer. Semin Cell Dev Biol 98: 98-104, 2020.
38. Sung H, Ferlay J, Siegel RL, Laversanne M, Soerjomataram I, Jemal A and Bray F: Global cancer statistics 2020: GLOBOCAN estimates of incidence and mortality worldwide for 36 cancers in 185 countries. CA Cancer J Clin 71: 209-249, 2021.
39. Brenner H, Kloor M and Pox CP: Colorectal cancer. Lancet 383: 1490-1502, 2014.
40. Kuipers EJ, Grady WM, Lieberman D, Seufferlein T, Sung JJ, Boelens PG, van de Velde CJ and Watanabe T: Colorectal cancer. Nat Rev Dis Primers 1: 15065, 2015.
41. Luengo A, Gui DY and Vander Heiden MG: Targeting metabolism for cancer therapy. Cell Chem Biol 24: 1161-1180, 2017.
42. Li J, Eu JQ, Kong LR, Wang L, Lim YC, Goh BC and Wong ALA: Targeting metabolism in cancer cells and the tumour microenvironment for cancer therapy. Molecules 25: 4831, 2020.
43. Galluzzi L, Kepp O, Vander Heiden MG and Kroemer G: Metabolic targets for cancer therapy. Nat Rev Drug Discov 12: 829-846, 2013.
44. Shah AN, Alam MM, Cao T and Zhang L: The role of ribosomes in mediating hypoxia response and tolerance in Eukaryotes. Nova Science Publishers, Inc. ISBN: 978-1-62417-698-2, 2013.
45. Staudacher JJ, Naarmann-de Vries IS, Ujvari SJ, Klinger B, Kasim M, Benko E, Ostareck-Lederer A, Ostareck DH, Bondke Persson A, Lorenzen S, *et al*: Hypoxia-induced gene expression results from selective mRNA partitioning to the endoplasmic reticulum. Nucleic Acids Res 43: 3219-3236, 2015.
46. Ivanova IG, Park CV and Kenneth NS: Translating the hypoxic response-the role of HIF protein translation in the cellular response to low oxygen. Cells 8: 114, 2019.
47. Chee NT, Lohse I and Brothers SP: mRNA-to-protein translation in hypoxia. Mol Cancer 18: 49, 2019.
48. Sanchez-Martin C, Serapian SA, Colombo G and Rasola A: Dynamically shaping chaperones. allosteric modulators of HSP90 family as regulatory tools of cell metabolism in neoplastic progression. Front Oncol 10: 1177, 2020.
49. Costantino E, Maddalena F, Calise S, Piscazzi A, Tirino V, Fersini A, Ambrosi A, Neri V, Esposito F and Landriscina M: TRAP1, a novel mitochondrial chaperone responsible for multi-drug resistance and protection from apoptotis in human colorectal carcinoma cells. Cancer Lett 279: 39-46, 2009.

50. Van de Wetering M, Francies HE, Francis JM, Bounova G, Iorio F, Pronk A, van Houdt W, van Gorp J, Taylor-Weiner A, Kester L, *et al*: Prospective derivation of a living organoid biobank of colorectal cancer patients. Cell 161: 933-945, 2015.
51. Sachs N, de Ligt J, Kopper O, Gogola E, Bounova G, Weeber F, Balgobind AV, Wind K, Gracanin A, Begthel H, *et al*: A living biobank of breast cancer organoids captures disease heterogeneity. Cell 172: 373-386 e10, 2018.
52. Yan HHN, Siu HC, Law S, Ho SL, Yue SSK, Tsui WY, Chan D, Chan AS, Ma S, Lam KO, *et al*: A comprehensive human gastric cancer organoid biobank captures tumor subtype heterogeneity and enables therapeutic screening. Cell Stem Cell 23: 882-897. e11, 2018.
53. Aggarwal V, Miranda O, Johnston PA and Sant S: Three dimensional engineered models to study hypoxia biology in breast cancer. Cancer Lett 490: 124-142, 2020.
54. Qiu GZ, Jin MZ, Dai JX, Sun W, Feng JH and Jin WL: Reprogramming of the tumor in the hypoxic niche: The emerging concept and associated therapeutic strategies. Trends Pharmacol Sci 38: 669-686, 2017.
55. Marhold M, Tomasich E, El-Gazzar A, Heller G, Spittler A, Horvat R, Krainer M and Horak P: HIF1α regulates mTOR signaling and viability of prostate cancer stem cells. Mol Cancer Res 13: 556-564, 2015.
56. Tan VP and Miyamoto S: Nutrient-sensing mTORC1: Integration of metabolic and autophagic signals. J Mol Cell Cardiol 95: 31-41, 2016.
57. Chun Y and Kim J: AMPK-mTOR signaling and cellular adaptations in hypoxia. Int J Mol Sci 22: 9765, 2021.
58. Melick CH, Meng D and Jewell JL: A-kinase anchoring protein 8L interacts with mTORC1 and promotes cell growth. J Biol Chem 295: 8096-8105, 2020.
59. Amin AG, Jeong SW, Gillick JL, Sursal T, Murali R, Gandhi CD and Jhanwar-Uniyal M: Targeting the mTOR pathway using novel ATP-competitive inhibitors, Torin1, Torin2 and XL388, in the treatment of glioblastoma. Int J Oncol 59: 83, 2021.
60. Morita M, Gravel SP, Hulea L, Larsson O, Pollak M, St-Pierre J and Topisirovic I: mTOR coordinates protein synthesis, mitochondrial activity and proliferation. Cell Cycle 14: 473-480, 2015.
61. Hannan KM, Sanij E, Hein N, Hannan RD and Pearson RB: Signaling to the ribosome in cancer-it is more than just mTORC1. IUBMB Life 63: 79-85, 2011.
62. Iadevaia V, Liu R and Proud CG: mTORC1 signaling controls multiple steps in ribosome biogenesis. Semin Cell Dev Biol 36: 113-120, 2014.
63. Tee AR: The target of rapamycin and mechanisms of cell growth. Int J Mol Sci 19: 880, 2018.
64. Gentilella A, Kozma SC and Thomas G: A liaison between mTOR signaling, ribosome biogenesis and cancer. Biochim Biophys Acta 1849: 812-820, 2015.
65. Valvezan AJ, Turner M, Belaid A, Lam HC, Miller SK, McNamara MC, Baglini C, Housden BE, Perrimon N, Kwiatkowski DJ, *et al*: mTORC1 couples nucleotide synthesis to nucleotide demand resulting in a targetable metabolic vulnerability. Cancer Cell 32: 624-638.e5, 2017.
66. Pelletier J, Thomas G and Volarević S: Ribosome biogenesis in cancer: New players and therapeutic avenues. Nat Rev Cancer 18: 51-63, 2018.
67. Chaillou T, Kirby TJ and McCarthy JJ: Ribosome biogenesis: Emerging evidence for a central role in the regulation of skeletal muscle mass. J Cell Physiol 229: 1584-1594, 2014.
68. Chen L, Xu B, Liu L, Liu C, Luo Y, Chen X, Barzegar M, Chung J and Huang S: Both mTORC1 and mTORC2 are involved in the regulation of cell adhesion. Oncotarget 6: 7136-7150, 2015.
69. Rad E, Murray JT and Tee AR: Oncogenic signalling through mechanistic target of rapamycin (mTOR): A driver of metabolic transformation and cancer progression. Cancers (Basel) 10: 5, 2018.
70. Yeh HS and Yong J: mTOR-coordinated post-transcriptional gene regulations: From fundamental to pathogenic insights. J Lipid Atheroscler 9: 8-22, 2020.
71. Matassa DS, Amoroso MR, Agliarulo I, Maddalena F, Sisinni L, Paladino S, Romano S, Romano MF, Sagar V, Loreni F, *et al*: Translational control in the stress adaptive response of cancer cells: A novel role for the heat shock protein TRAP1. Cell Death Dis 4: e851, 2013.
72. Sisinni L, Maddalena F, Lettini G, Condelli V, Matassa DS, Esposito F and Landriscina M: TRAP1 role in endoplasmic reticulum stress protection favors resistance to anthracyclins in breast carcinoma cells. Int J Oncol 44: 573-582, 2014.
73. Amoroso MR, Matassa DS, Laudiero G, Egorova AV, Polishchuk RS, Maddalena F, Piscazzi A, Paladino S, Sarnataro D, Garbi C, *et al*: TRAP1 and the proteasome regulatory particle TBP7/Rpt3 interact in the endoplasmic reticulum and control cellular ubiquitination of specific mitochondrial proteins. Cell Death Differ 19: 592-604, 2012.
74. Matassa DS, Agliarulo I, Amoroso MR, Maddalena F, Sepe L, Ferrari MC, Sagar V, D'Amico S, Loreni F, Paolella G, *et al*: TRAP1-dependent regulation of p70S6K is involved in the attenuation of protein synthesis and cell migration: Relevance in human colorectal tumors. Mol Oncol 8: 1482-1494, 2014.
75. Delprato A, Al Kadri Y, Pérébaskine N, Monfoulet C, Henry Y, Henras AK and Fribourg S: Crucial role of the Rcl1p-Bms1p interaction for yeast pre-ribosomal RNA processing. Nucleic Acids Res 42: 10161-10172, 2014.
76. Kharde S, Calviño FR, Gumiero A, Wild K and Sinning I: The structure of Rpf2-Rrs1 explains its role in ribosome biogenesis. Nucleic Acids Res 43: 7083-7095, 2015.
77. Turowski TW and Tollervey D: Cotranscriptional events in eukaryotic ribosome synthesis. Wiley Interdiscip Rev RNA 6: 129-139, 2015.
78. Wang Y, Zhu Q, Huang L, Zhu Y, Chen J, Peng J and Lo LJ: Interaction between Bms1 and Rcl1, two ribosome biogenesis factors, is evolutionally conserved in zebrafish and human. J Genet Genomics 43: 467-469, 2016.
79. Kornprobst M, Turk M, Kellner N, Cheng J, Flemming D, Koš-Braun I, Koš M, Thoms M, Berninghausen O, Beckmann R and Hurt E: Architecture of the 90S pre-ribosome: A structural view on the birth of the eukaryotic ribosome. Cell 166: 380-393, 2016.
80. Sun Q, Zhu X, Qi J, An W, Lan P, Tan D, Chen R, Wang B, Zheng S, Zhang C, *et al*: Correction: Molecular architecture of the 90S small subunit pre-ribosome. Elife 6: e29876, 2017.
81. Chaker-Margot M, Barandun J, Hunziker M and Klinge S: Architecture of the yeast small subunit processome. Science 355: eaal1880, 2017.
82. Boissier F, Schmidt CM, Linnemann J, Fribourg S and Perez-Fernandez J: Pwp2 mediates UTP-B assembly via two structurally independent domains. Sci Rep 7: 3169, 2017.
83. Zhao S, Chen Y, Chen F, Huang D, Shi H, Lo LJ, Chen J and Peng J: Sas10 controls ribosome biogenesis by stabilizing Mpp10 and delivering the Mpp10-Imp3-Imp4 complex to nucleolus. Nucleic Acids Res 47: 2996-3012, 2019.
84. Scaiola A, Peña C, Melanie Weisser M, Böhringer D, Leibundgut M, Klingauf-Nerurkar P, Gerhardy S, Panse VG and Ban N: Structure of a eukaryotic cytoplasmic pre-40S ribosomal subunit. EMBO J 37: e98499, 2018.
85. Sá-Moura B, Kornprobst M, Kharde S, Ahmed YL, Stier G, Kunze R, Sinning I and Hurt E: Correction: Mpp10 represents a platform for the interaction of multiple factors within the 90S pre-ribosome. PLoS One 15: e0234932, 2020.